Supplement of Atmos. Chem. Phys., 26, 6165–6196, 2026
https://doi.org/10.5194/acp-26-6165-2026-supplement

Atmospheric Chemistry and Physics
Open Access

Supplement of

Tropospheric bromine monoxide in Ny-Ålesund: source analysis and impacts on atmospheric chemistry

Qidi Li et al.

Correspondence to: Yuhan Luo (yhluo@aiofm.ac.cn) and Xin Yang (xinyang55@bas.ac.uk)

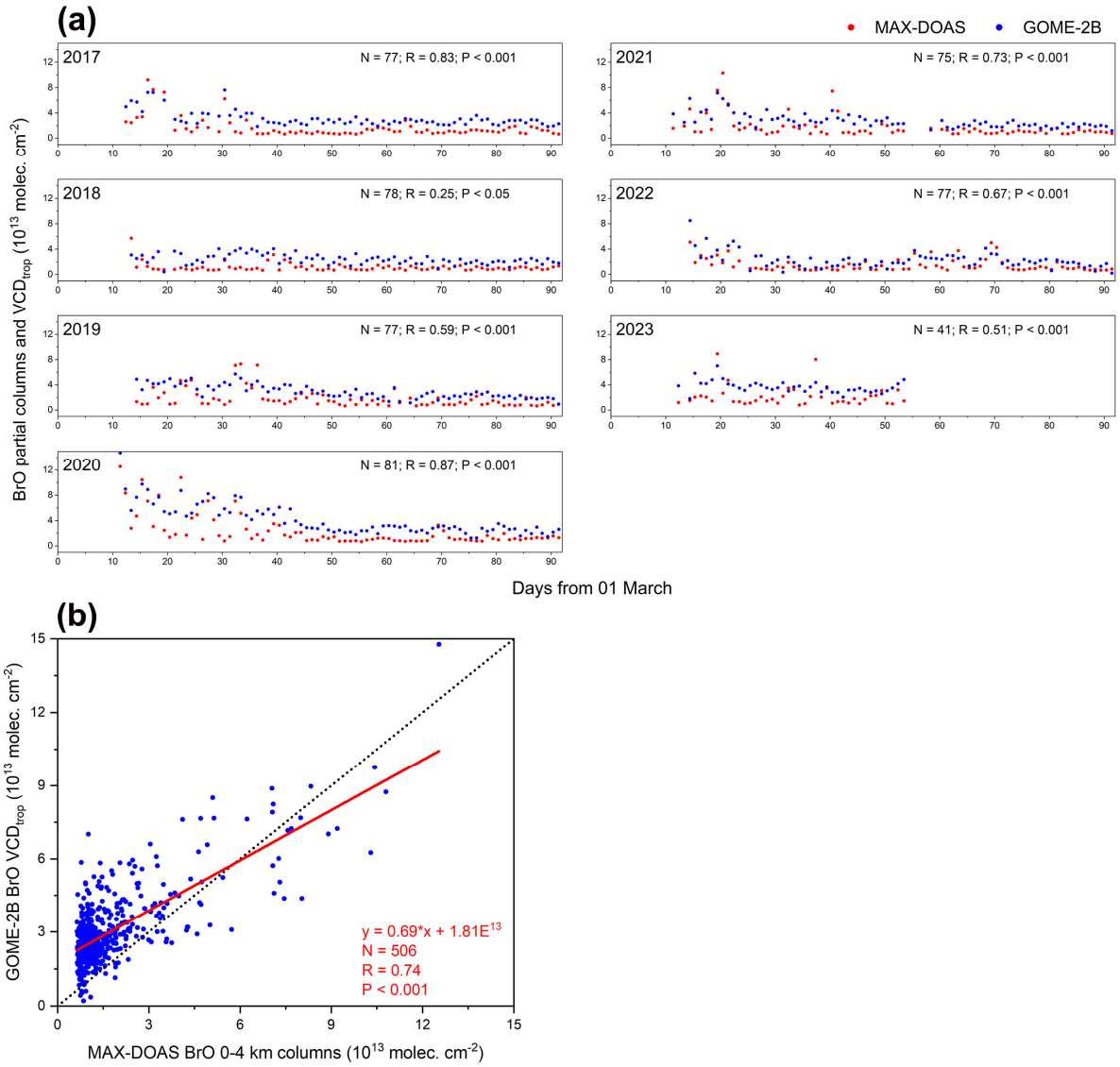

Figure S1. Daily time series of MAX-DOAS BrO partial columns (red symbols) in Ny-Ålesund and GOME-2B tropospheric BrO columns (blue symbols) within 45 km of Ny-Ålesund from March to May between 2017 and 2023 (a), and their correlation over the entire period (b). Note: Daily averages are calculated using only the hours with valid GOME-2B data, along with the corresponding MAX-DOAS observations for those hours.

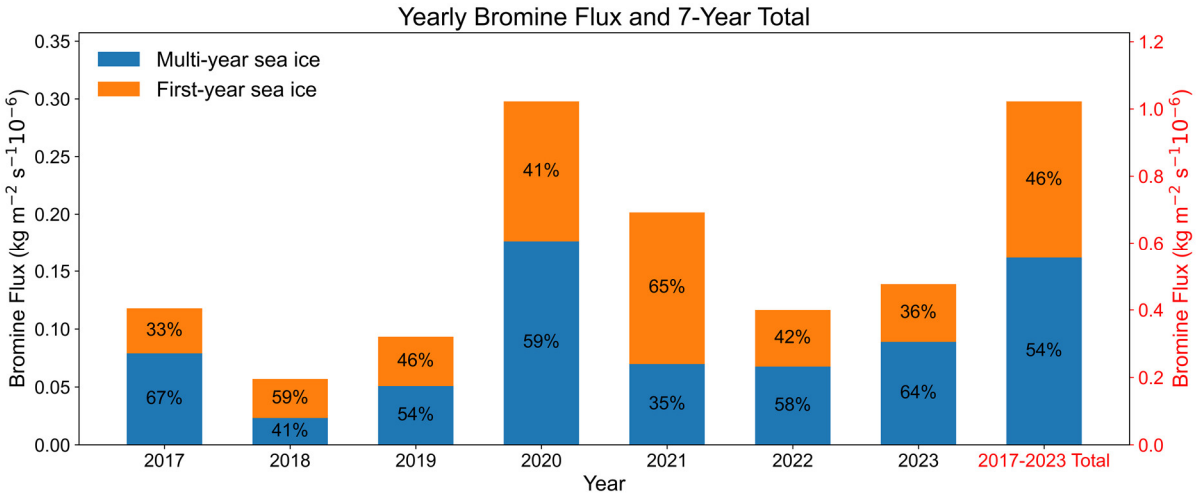

Figure S2. Yearly (March–May) and seven-year total blowing-snow-sourced bromine emission fluxes over MYI and FYI along backward trajectories of air masses arriving at Ny-Ålesund during BEEs. Blue and orange bars indicate the contributions from MYI and FYI, respectively.

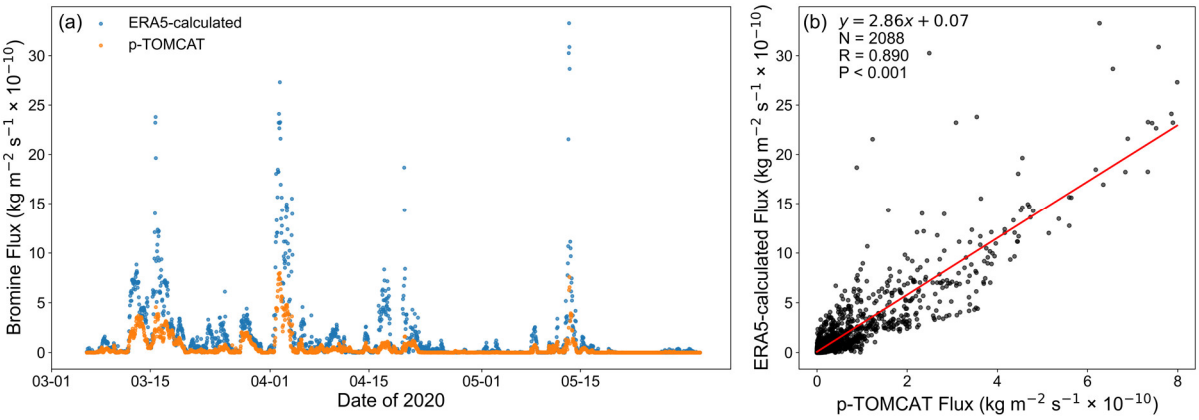

Figure S3. (a) Time series of blowing-snow-sourced bromine fluxes calculated from ERA5 meteorological fields (blue dots) and from the p-TOMCAT (orange dots) during March–May 2020. The fluxes are summed over the 0–3 km layer and shown at hourly resolution. (b) Scatter plot showing the correlation between the ERA5-calculated and p-TOMCAT-simulated blowing-snow-sourced bromine fluxes over the same period.

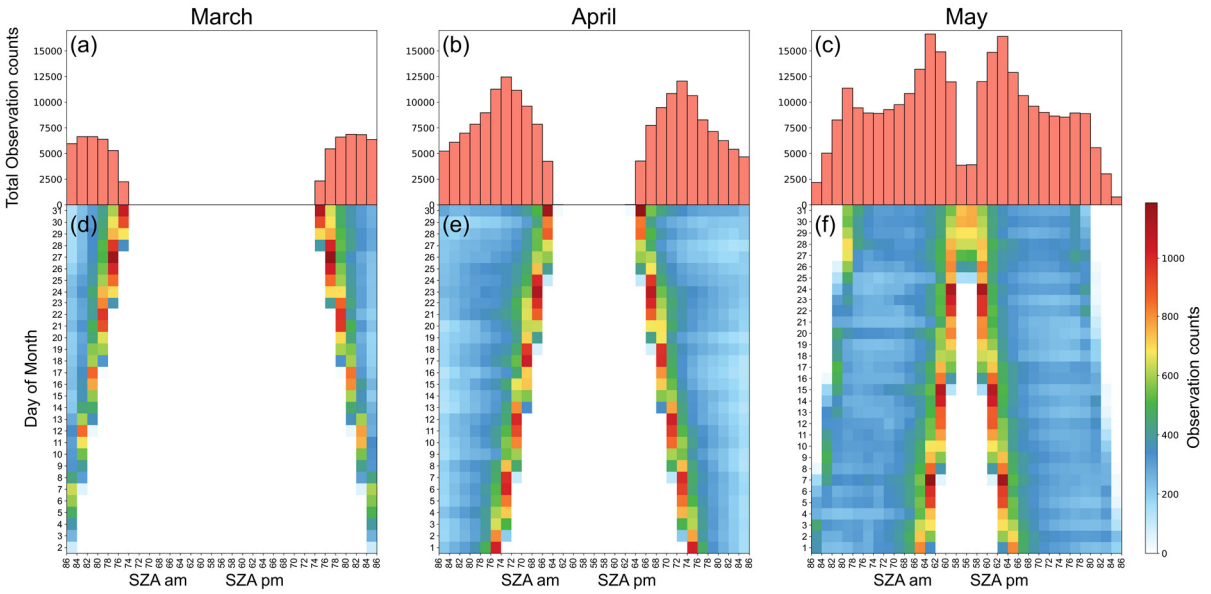

Figure S4. SZA distributions sampled at the times of MAX-DOAS measurements during March (a, d), April (b, e), and May (c, f) in 2017–2023. Panels (a–c) show the total number of observations aggregated across all years as a function of SZA for morning (AM) and afternoon (PM) conditions, while panels (d–f) present the corresponding daily SZA frequency distributions. March and April are characterized by a single peak at large SZA, whereas May exhibits clear double peaks.

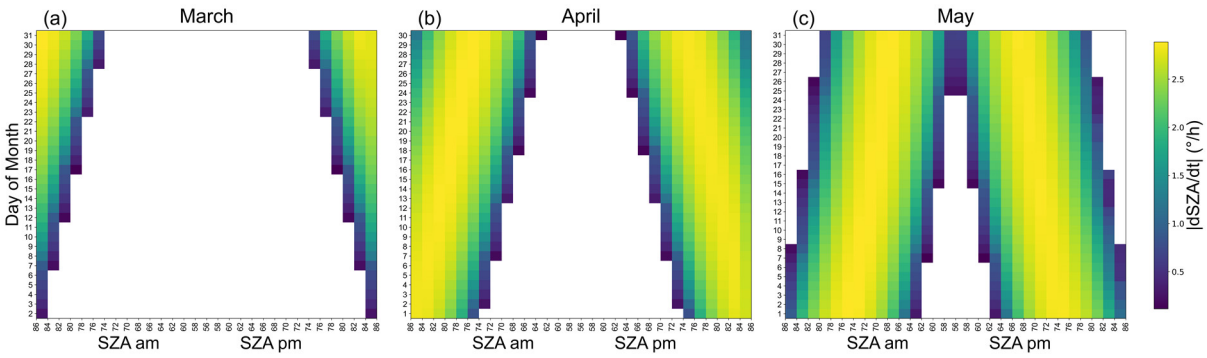

Figure S5. Absolute SZA variation rates (|dSZA/dt|, °/h) sampled at the times of MAX-DOAS measurements in March (a), April (b), and May (c) during 2017–2023. For each day, morning (AM) and afternoon (PM) observations are binned by SZA. Different colors represent the value of |dSZA/dt|, with lower values corresponding to slower SZA variation and higher values to faster SZA variation.

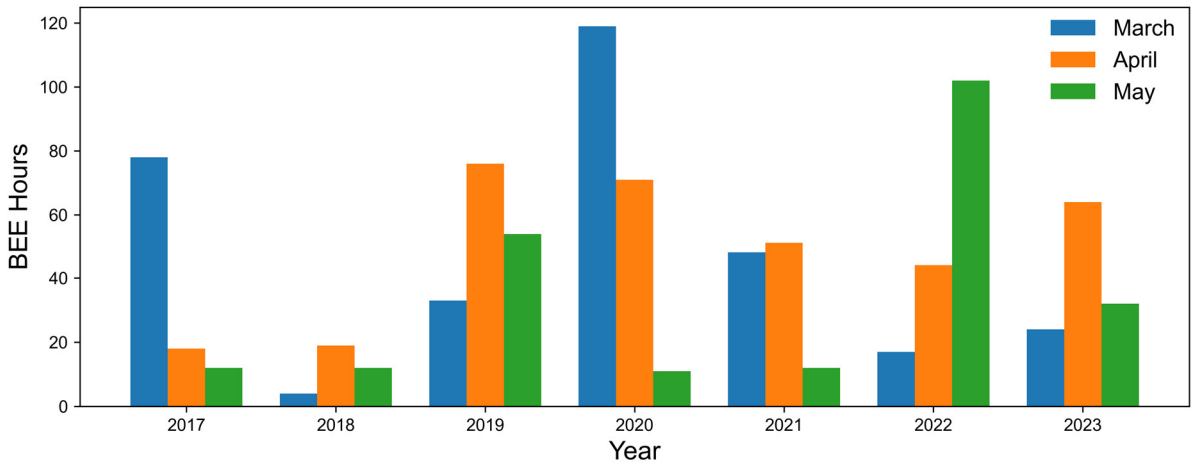

Figure S6. Monthly total hours of BEEs in Ny-Ålesund from March to May during 2017–2023. A BEE is defined as any hour during which BrO VMR exceeds 12 pptv at any altitude between 0 and 3 km.

Table S1. Percentage of air-mass contact time (along the 5-d trajectories) with the free troposphere, land, sea ice, and open ocean for all BEEs that occurred in March, April and May during 2017–2023. N in the bracket represents the cumulative total of hours for air masses in each 200 m altitude interval within the 0–3 km range. Note that the boundary layer height is set to 500 m.

	Percentage of Contact Time during BEEs			
	March (N=879)	April (N=835)	May (N=445)	Total (N=2159)
Free	35.69%	32.82%	36.98%	34.85%
Land	6.21%	7.95%	3.50%	6.32%
Sea ice	54.74%	50.88%	48.75%	52.01%
Ocean	3.36%	8.35%	10.77%	6.82%

Table S2. The same as Table S1, but with the boundary layer height set to 1000 m.

	Percentage of Contact Time during BEEs			
	March (N=879)	April (N=835)	May (N=445)	Total (N=2159)
Free	14.30%	13.54%	15.47%	14.25%
Land	10.91%	14.15%	6.28%	11.21%
Sea ice	70.25%	61.99%	64.74%	65.92%
Ocean	4.54%	10.32%	13.51%	8.62%

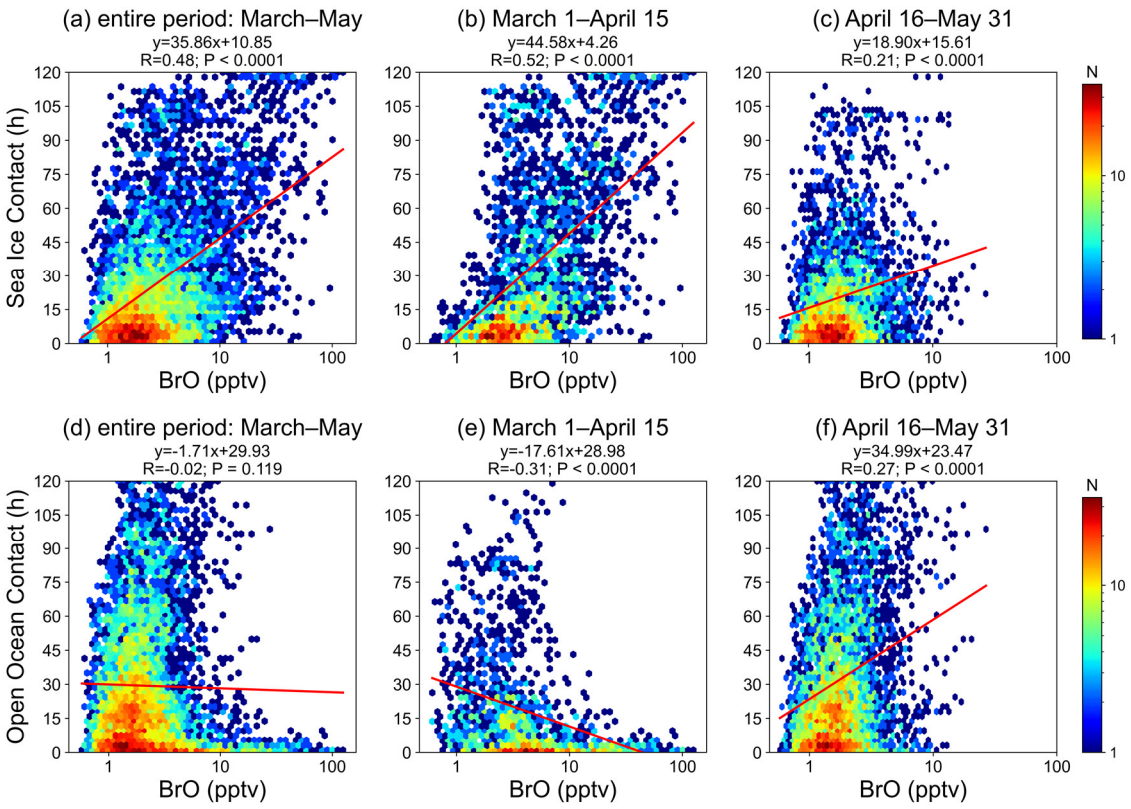

Figure S7. Correlation analysis between BrO VMR and surface contact times over sea ice and open ocean in 2020. Panels (a–c) show the correlation between BrO VMR and sea-ice contact time: (a) for the entire period from March to May, (b) for the first half of the period (March 1–April 15), and (c) for the second half (April 16–May 31). Panels (d–f) show the correlation between BrO VMR and open-ocean contact time: (d) for the entire period, (e) for the first half, and (f) for the second half.

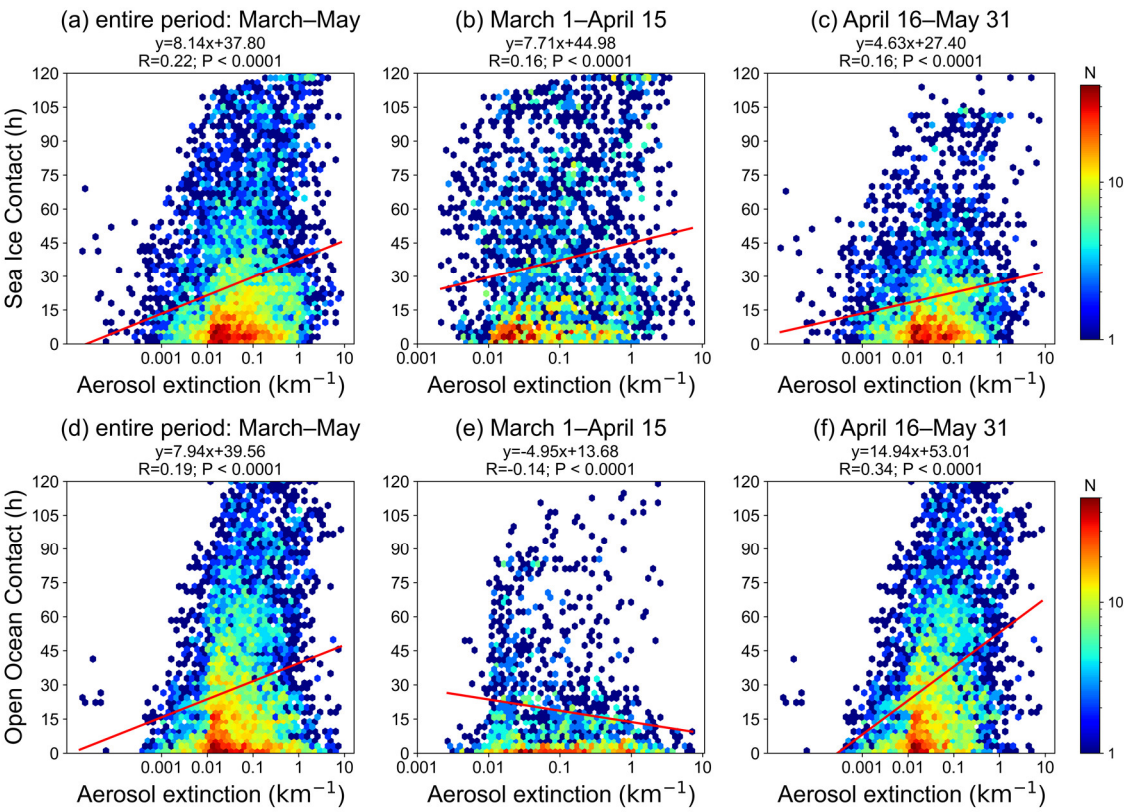

Figure S8. Correlation analysis between aerosol extinction and surface contact times over sea ice and open ocean in 2020. Panels (a–c) show the correlation between aerosol extinction and sea-ice contact time: (a) for the entire period from March to May, (b) for the first half of the period (March 1–April 15), and (c) for the second half (April 16–May 31). Panels (d–f) show the correlation between aerosol extinction and open-ocean contact time: (d) for the entire period, (e) for the first half, and (f) for the second half.

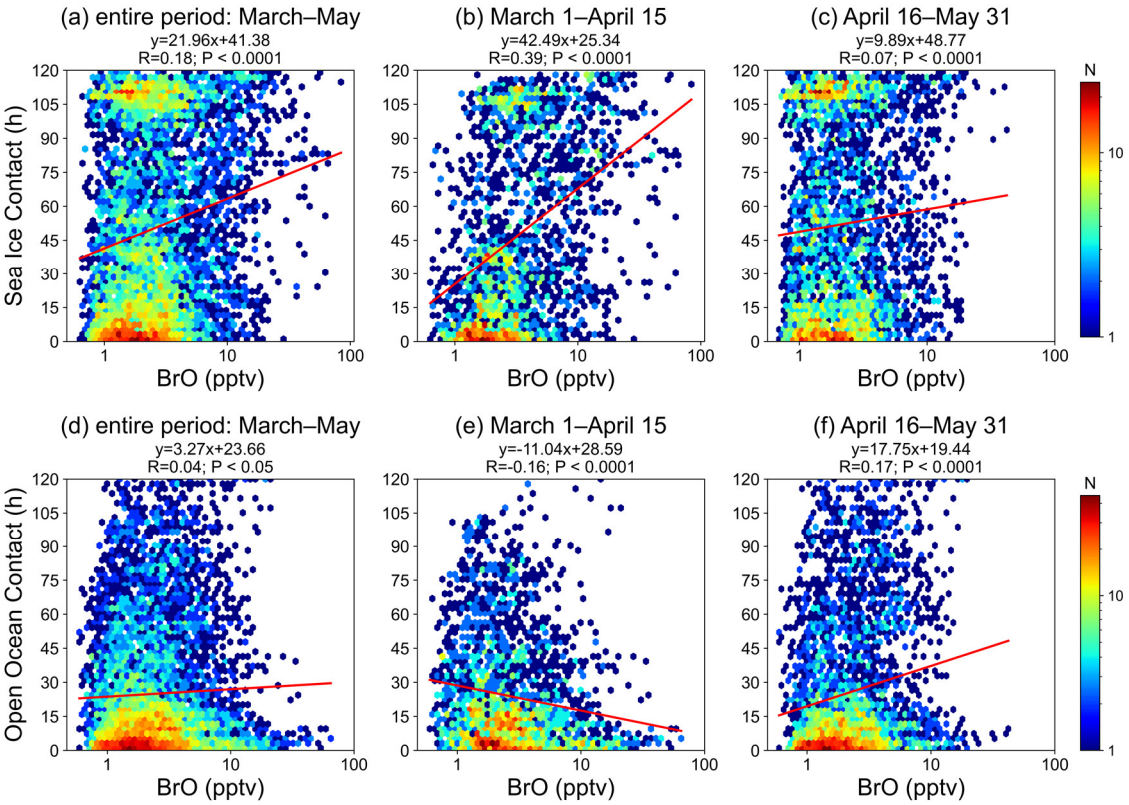

Figure S9. Same as Fig. 7, but for 2019.

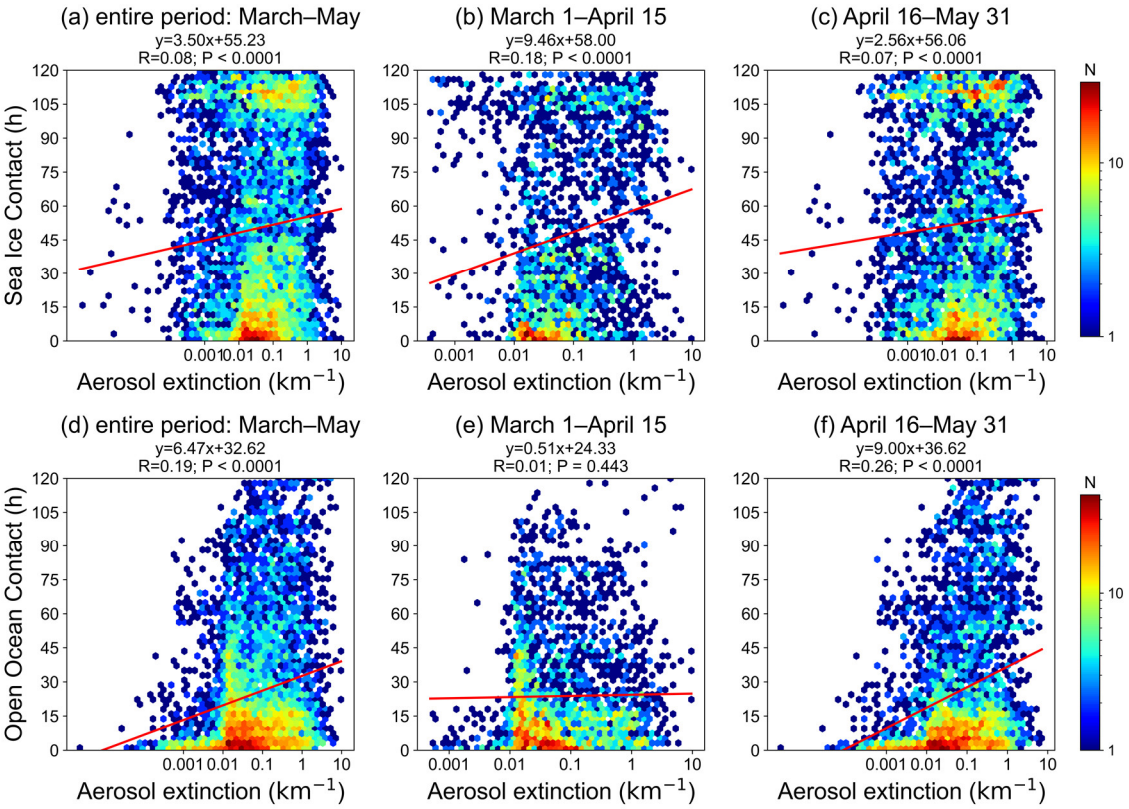

Figure S10. Same as Fig. 8, but for 2019.

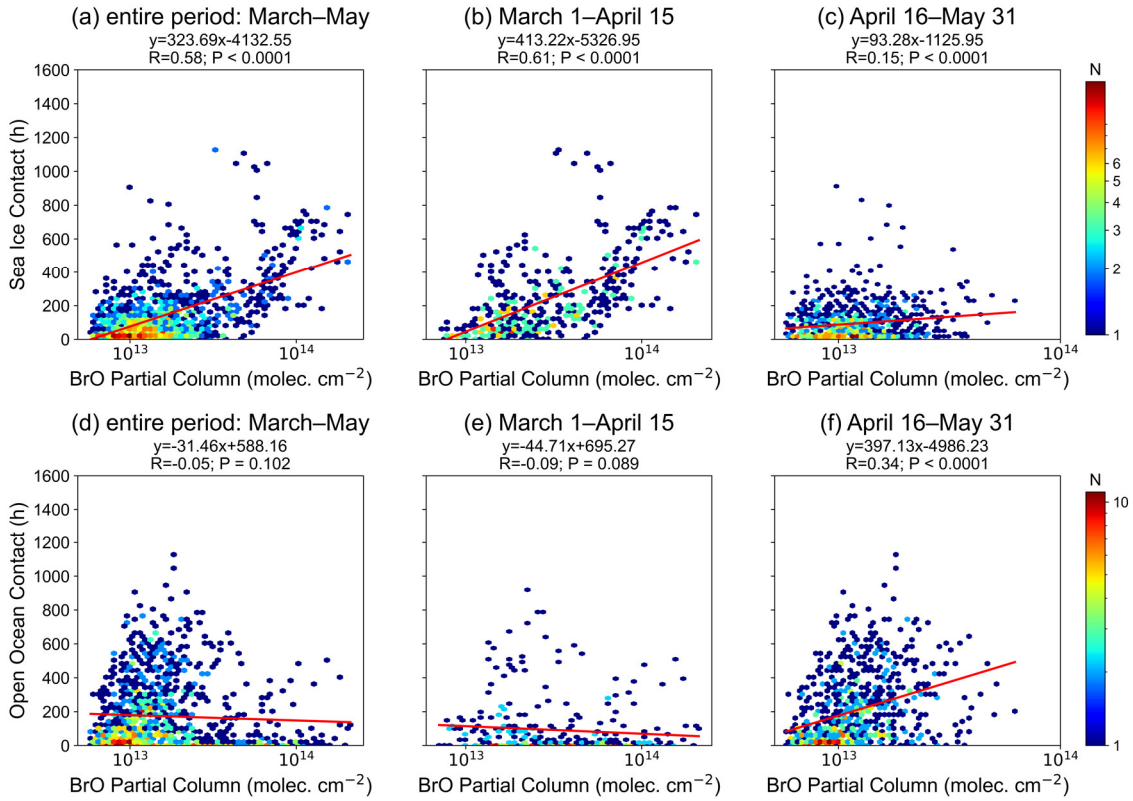

Figure S11. Correlation analysis between BrO partial column and total surface contact time summed over 15 vertical levels (0–3 km) for sea ice and open ocean in 2020. Panels (a–c) show the correlation between BrO partial column and total sea-ice contact time: (a) for the entire period from March to May, (b) for the first half of the period (March 1–April 15), and (c) for the second half (April 16–May 31). Panels (d–f) show the correlation between BrO partial column and total open-ocean contact time: (d) for the entire period, (e) for the first half, and (f) for the second half.

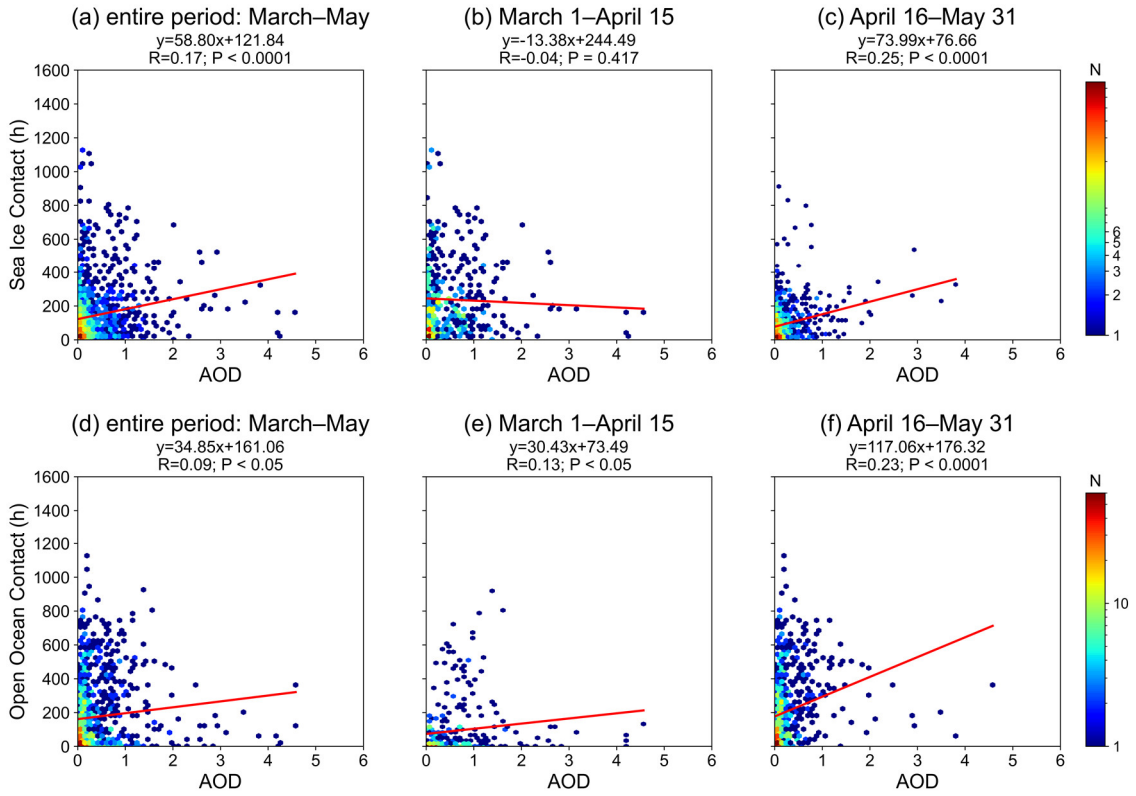

Figure S12. Correlation analysis between AOD and total surface contact time summed over 15 vertical levels (0–3 km) for sea ice and open ocean in 2020. Panels (a–c) show the correlation between AOD and total sea-ice contact time: (a) for the entire period from March to May, (b) for the first half of the period (March 1–April 15), and (c) for the second half (April 16–May 31). Panels (d–f) show the correlation between AOD and total open-ocean contact time: (d) for the entire period, (e) for the first half, and (f) for the second half.

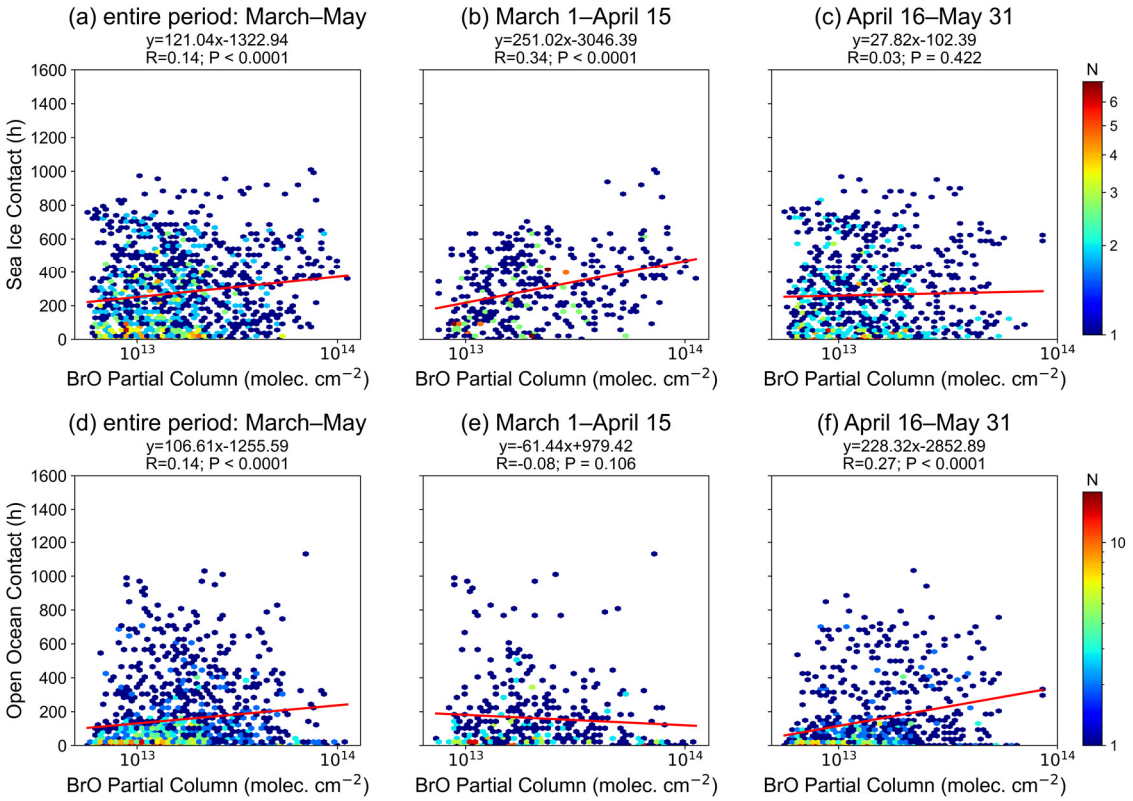

Figure S13. Same as Fig. 11, but for 2019.

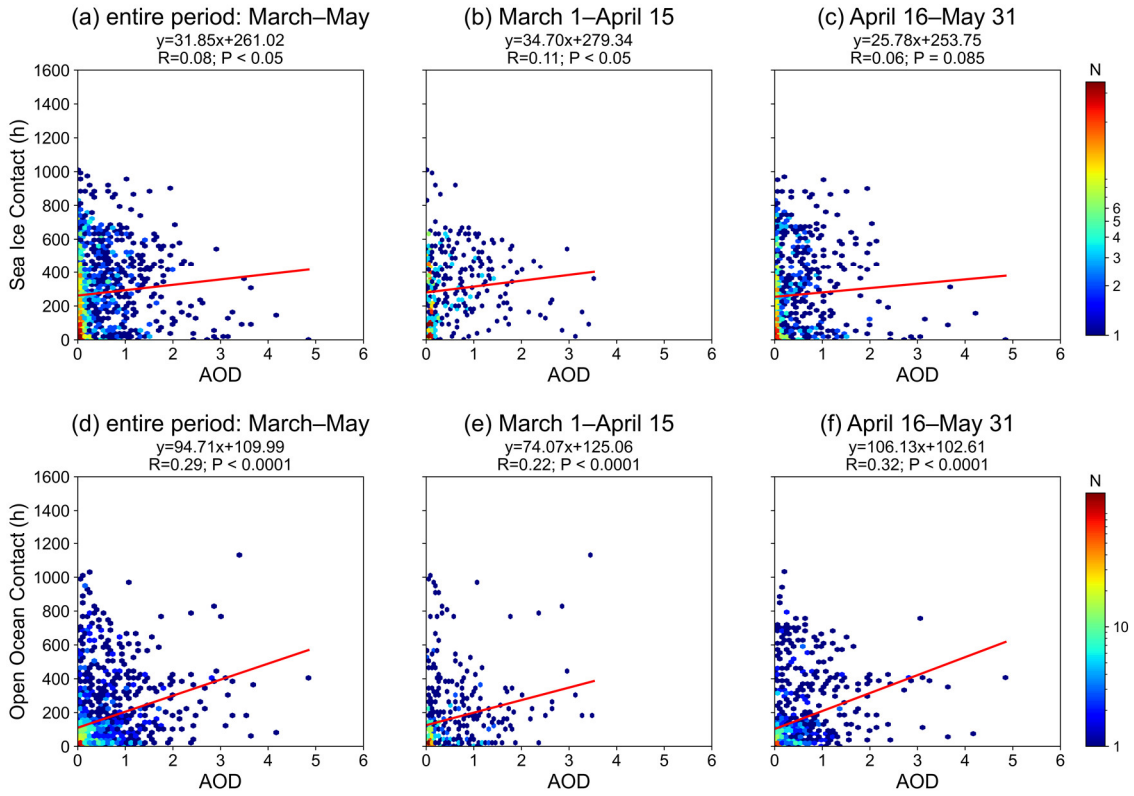

Figure S14. Same as Fig. 12, but for 2019.

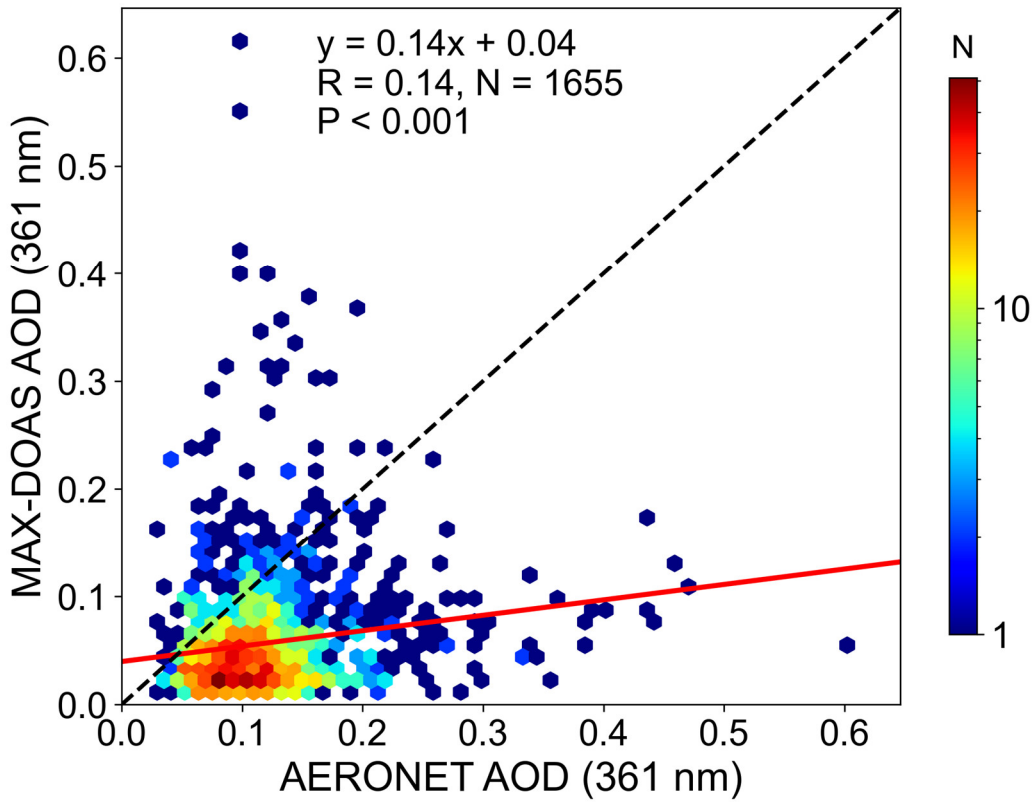

Figure S15. Correlation analysis between MAX-DOAS AOD and AERONET AOD during March–May for the 2017–2023 period.

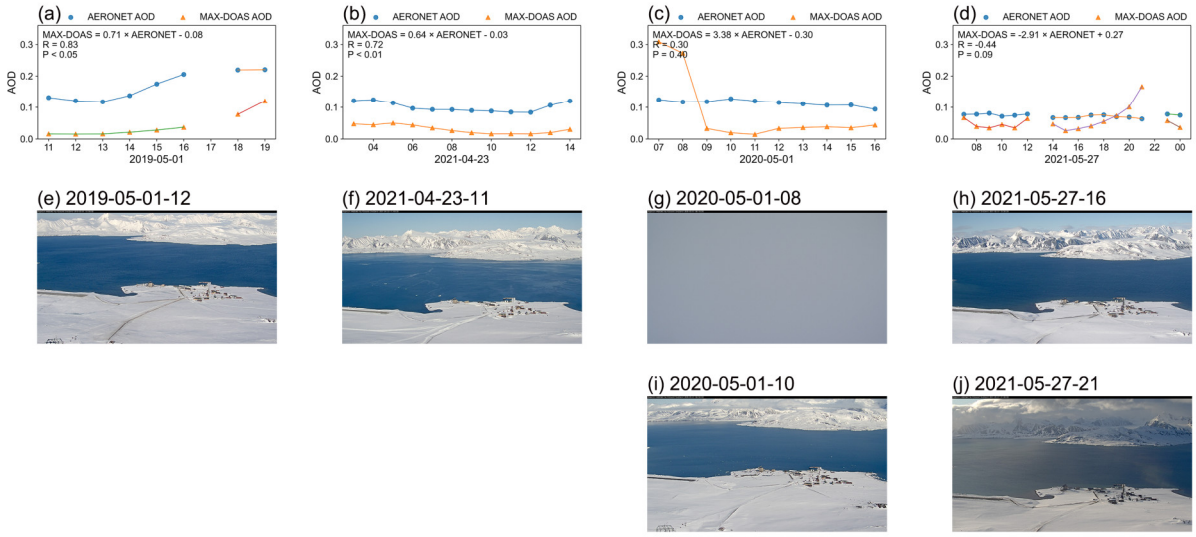

Figure S16. Time series of MAX-DOAS and AERONET AOD under clear-sky (a, b) and cloudy (c, d) conditions at Ny-Ålesund. Panels (e)–(j) show camera images taken at Ny-Ålesund on the corresponding days. All times are given in UTC.

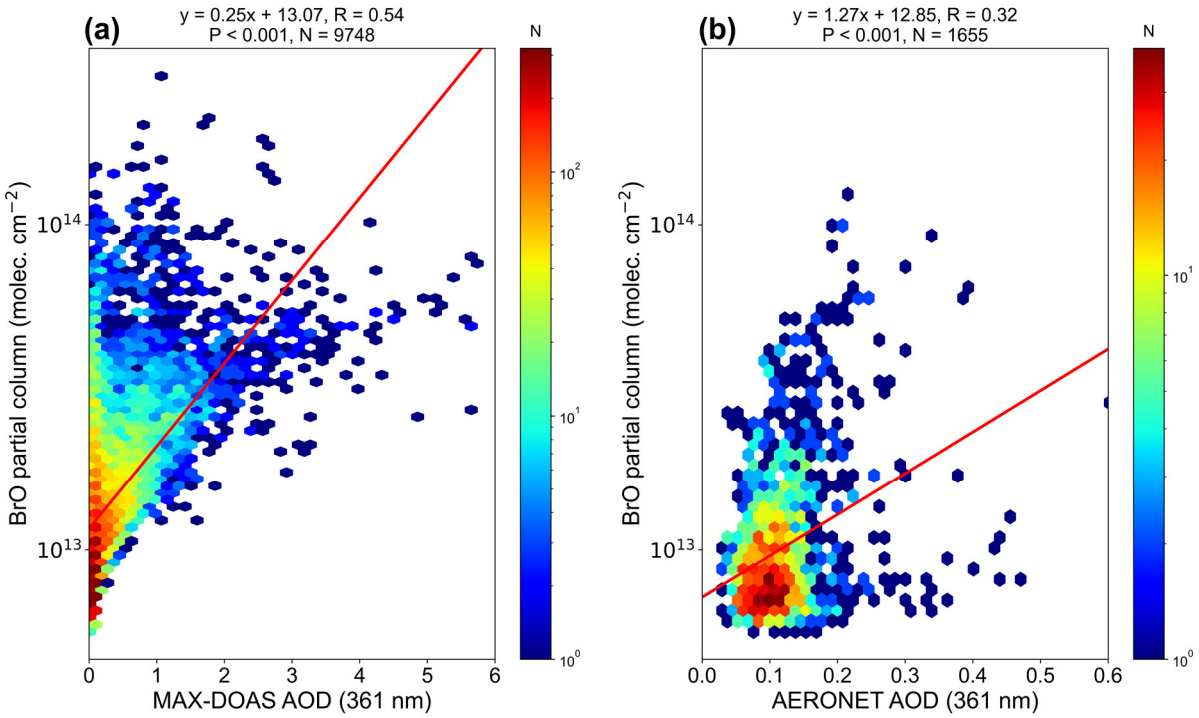

Figure S17. Correlation analysis between MAX-DOAS BrO partial columns and MAX-DOAS AOD (a) and AERONET AOD (b) during March–May for the 2017–2023 period.

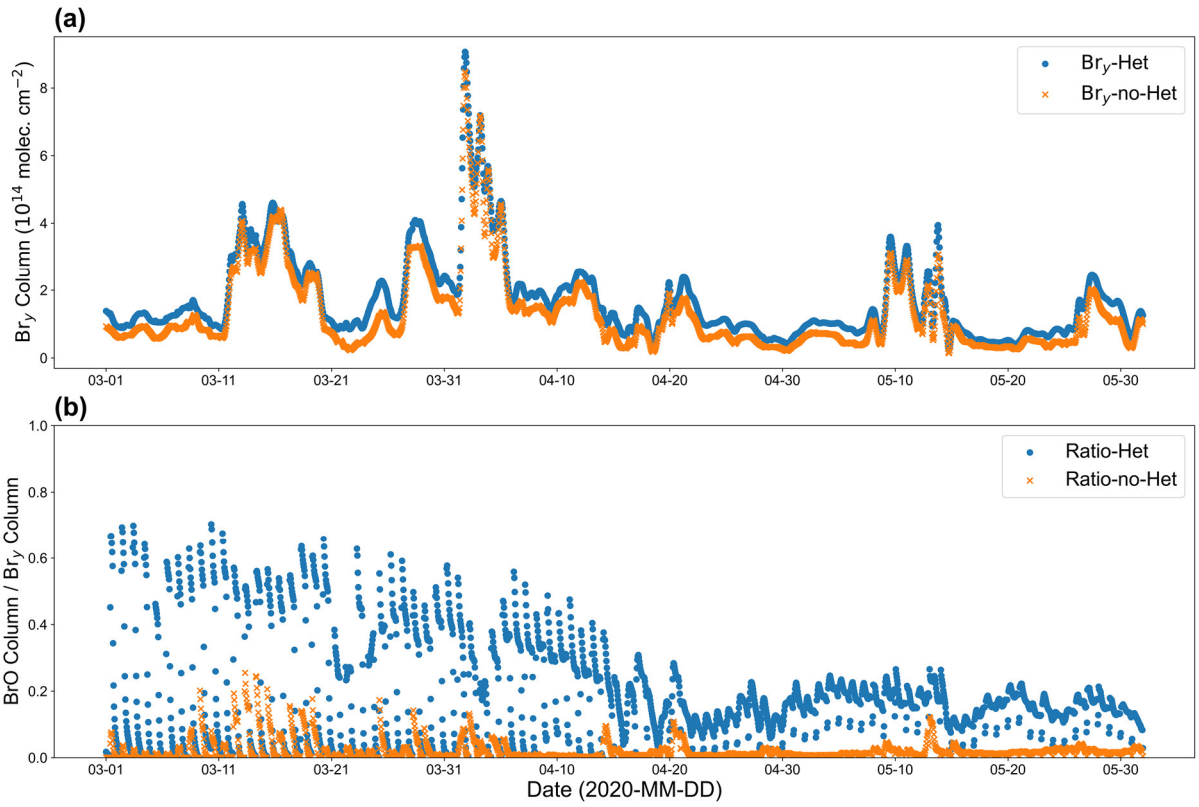

Figure S18. Time series during the March–May 2020 BEEs. (a) Simulated Br$_y$ partial column (0–4 km) with heterogeneous reactivation (blue) and without heterogeneous reactivation (orange). (b) Simulated BrO (0–4 km) to Br$_y$ (0–4 km) partial column ratio for the two experiments.

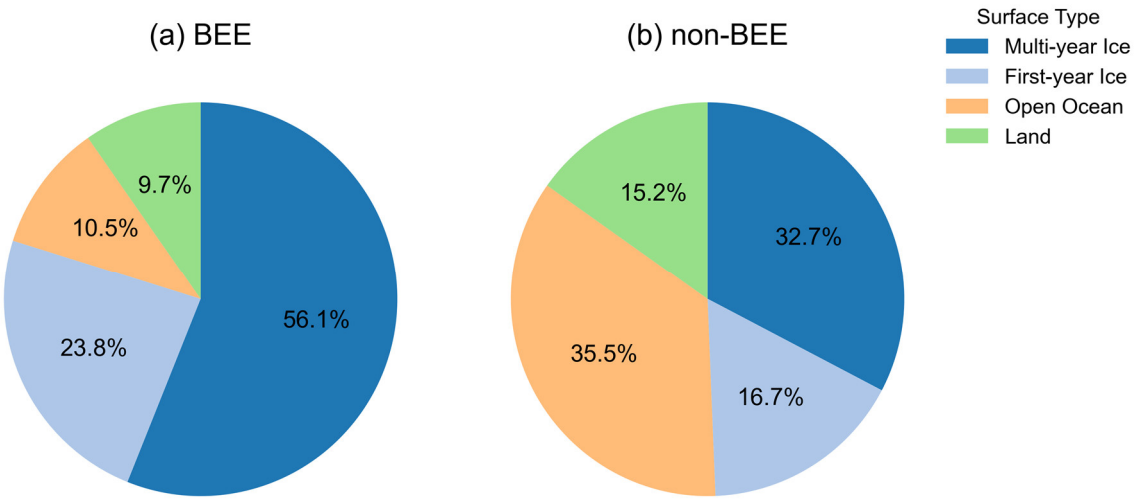

Figure S19. Percentages of air masses associated with (a) BEE and (b) non-BEE events that contact with different surface types (< 500 m) during March–May in 2017–2023. Note that the free troposphere is excluded.

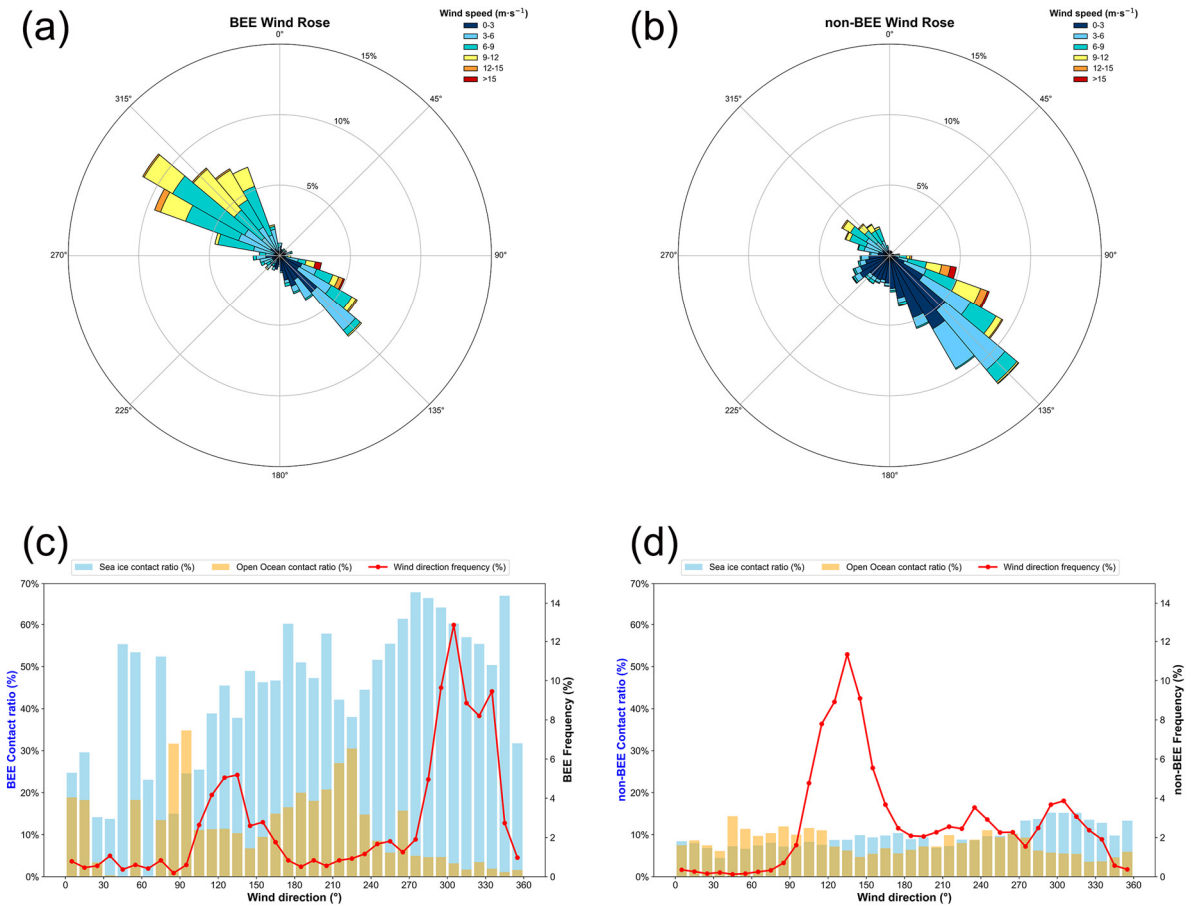

Figure S20. Wind rose diagrams for BEE (a) and non-BEE (b) during March–May, based on wind speed and direction measured in Ny-Ålesund from 2017 to 2023. Panels (c) and (d) present, for BEE and non-BEE periods respectively, the wind direction frequency (red line) along with the mean 5-day back-trajectory contact ratios with sea ice (blue bars) and open ocean (yellow bars) for each wind sector.

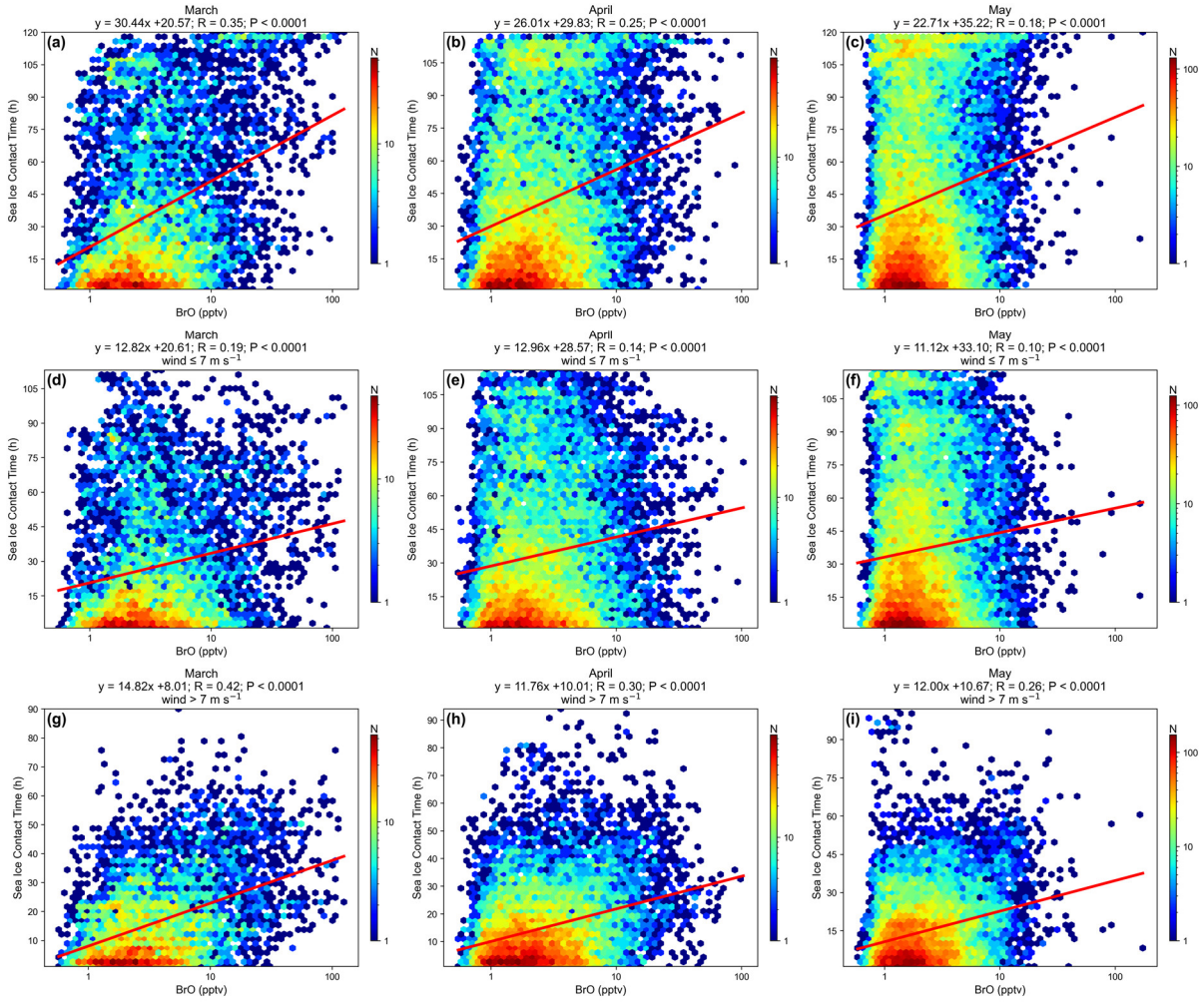

Figure S21. Correlation analysis of BrO VMR (0–3 km altitude) with sea-ice contact time from March to May during 2017–2023. (a–c) Correlations between BrO and overall sea-ice contact time; (d–f) Correlations between BrO and sea-ice contact time during low wind speed conditions (wind ≤ 7 m/s); (g–i) Correlations between BrO and sea-ice contact time during high wind speed conditions (wind > 7 m/s).

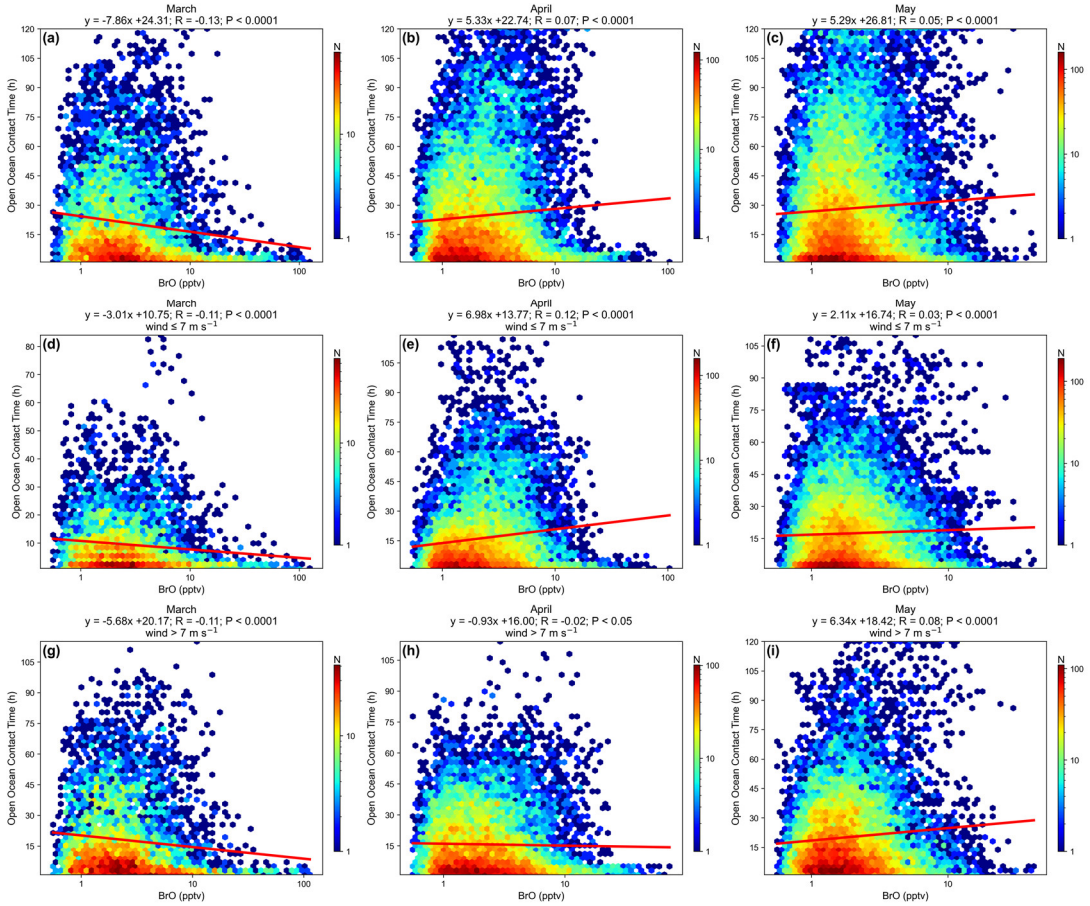

Figure S22. Correlation analysis of BrO VMR (0–3 km altitude) with open-ocean contact time from March to May during 2017–2023. (a–c) Correlations between BrO and overall open-ocean contact time; (d–f) Correlations between BrO and open-ocean contact time during low wind speed conditions (wind ≤ 7 7 m s^{-1}); (g–i) Correlations between BrO and open-ocean contact time during high wind speed conditions (wind > 7 m s^{-1}).